

# Numerical simulations of nonequilibrium and diffusive effects in spherical shock waves

V.V. Riabov

## 1 Introduction: Relaxation effects in expanding gas flows

Experimental studies of underexpanded  $N_2$  jets [1], [2] discovered a delay of rotational temperature  $T_R$  compared to the translational one  $T_t$ . A drop in the gas density downstream leads to a decrease in the number of collisions and the  $T_R$  departure from the equilibrium value [3], [4]. Another cause for the  $T_R$  departure [5] could be explained in terms of quantum concepts. Because of the  $T_t$  plunge, the adiabatic collision conditions are realized at a certain temperature, rotational-transfer probabilities begin to decrease [6], and the relaxation time  $\tau_R$  increases. Calculations based on the classical concept [7], [8], [9] do not show a tendency of increasing  $\tau_R$  with the decrease of  $T_t$  under the adiabatic rotational energy exchange conditions. Computational results [4], [5], based on the quantum concept of energy exchange, correlate well with experimental data [2] of  $T_R$  distribution along the jet axis.

In the present study, the flow from a spherical source is used as the approximation model of the flow in underexpanded jets [4] and spherical shock waves. Rotational relaxation effects are analyzed by using the continuum approach and classical models [7] at  $T_t > 100$  K and quantum approach [5] at  $T_t < 100$  K. In addition, diffusive kinetic effects in spherical flows of Ar-He mixtures are studied. These effects are important in studies of separation processes in jets and physics of explosion.

## 2 Rotational relaxation effects in spherical shock waves

The full system of the Navier-Stokes equations and the relaxation equation, based on the  $\tau$ -approximation [9], has been solved by the implicit method [3]. Solutions depend on Reynolds number  $Re_*$ , pressure ratio  $P = p_0/p_a$ , temperature  $T_a$ , and re-

---

*Department of Computer Science, Rivier College  
420 S. Main St., Nashua, New Hampshire 03060 (USA)*

laxation parameter  $B_*$  that is calculated as a ratio of  $p\tau_R$  and viscosity. Here index "a" refers to background conditions and index \* refers to sonic conditions. Computations confirmed the delay [4] of  $T_R$  compared to  $T_t$ . The rate of  $T_R$  -decrease slows down with the gas expanding in the supersonic zone that leads to its "frozen" value. The R-T equilibrium never exists in front of the spherical shock. As the result of gas compression in the shock wave, rapid increase of  $T_R$  occurs. The values of  $T_t$  also begin to increase here, and reach the value of  $T_a$  behind the shock.

The distributions of  $T_R$  and  $T_t$  are shown in Fig. 1 (left). The same figure displays the influence of changes in pressure ratio P under the conditions  $Re_* = 161.83$ ,  $B_* = 28.4$ , and  $T_a = 295$  K. Inviscid flow parameters  $T_R$  and  $T_t$  were estimated in [5].

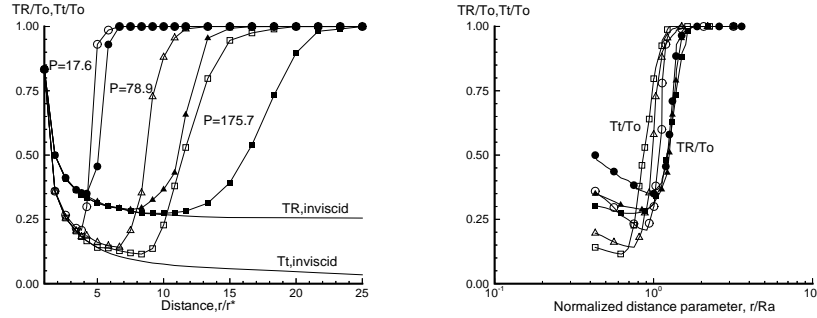


**Fig. 1** Left: Rotational  $T_R$  (filled markers) and translational  $T_t$  (empty markers) temperatures in spherical flow at various pressure ratios:  $P = 17.6$  (circles),  $78.9$  (triangles), and  $175.7$  (squares). Right:  $T_R$  and  $T_t$  at various parameters:  $K_2 = 38.6$  (circles),  $18.2$  (triangles), and  $12.2$  (squares)

The numerical analysis showed that the main factors that influence the relaxation process are  $B_*$  and the relaxation-time function. The decrease of  $B_*$  leads to a faster "frozen" value of  $T_R$  (see Fig. 2) in the supersonic-flow zone.

It has been found that the spherical flow could be separated by the coordinate  $R_S$ , at which the stream parameters are extreme, into two regions with different properties [10]. In the first "internal" region the flow is supersonic [4]. The flow parameters depend on the Reynolds numbers  $Re_*$  and  $Re_S$  (or related Knudsen numbers  $Kn_*$  and  $Kn_S$ ). The viscosity and thermal conductivity have a minor influence on the distribution of  $T_R$  and  $T_t$  in this region. The R-T relaxation effect dominates here.

In the second "external" region, there is a transition of supersonic flow through the spherical shock wave into a subsonic stream. The Reynolds number  $Re_a$  (or related Knudsen number  $Kn_a$ ) based on the length scale parameter at infinity,  $R_a$ , is the major similarity parameter in this region. The similarity factor  $K_2 = Re_a$  (introduced in [11], [12]) can be used to study the flow structure here:

$$K_2 = Re_*(p_a/p_{0*})^{0.5}; R_a = r_*(p_{0*}/p_a)^{0.5} \quad (1)$$

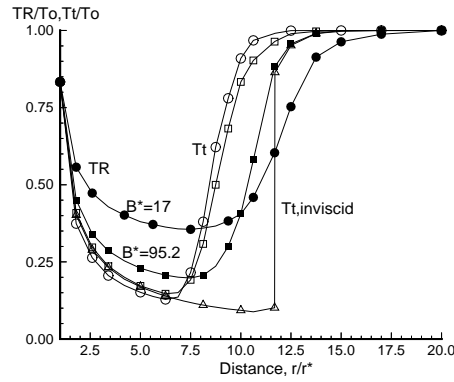


**Fig. 2** Rotational  $T_R$  (filled markers) and translational  $T_t$  (empty markers) temperatures in spherical flow as a function of relaxation parameter:  $B_* = 17$  (circles) and  $B_* = 95.2$  (squares)

The renormalized temperature characteristics of the spherical expanding nonequilibrium flow in the "external" region are shown in Fig. 1 (right). The major changes of  $T_R$  and  $T_t$  occur in the shock wave at values of the normalized distance parameter  $r/R_a$  about 1. The shock width decreases with increasing the parameter  $K_2$ .

### 3 Kinetic and diffusive effects in spherical shock waves

Kinetic and diffusion effects in Ar-He spherical expanding flows (mole fraction  $f_{Ar,*} = 0.5$ ) were studied using the direct simulation Monte Carlo method [13] at  $Kn_*$  from 0.0015 ( $Re_* = 1240$ ) to 0.015 ( $Re_* = 124$ ) and pressure ratios  $P$  from 100 to 10,000. Both phenomena influence the shock thickness, parallel and transverse species' temperatures, diffusive velocities, and species separation. Distributions of Ar mole fraction and species temperatures are shown in Fig. 3 at  $Kn_* = 0.015$  and various  $P = 100, 1000, \text{ and } 10000$  (filled squares, circles, and triangles).

The species concentration changes insignificantly in the supersonic region at  $r < R_a$ . Accumulation of the light component occurs in the spherical shock (see Fig. 3 (left)) due to baro-diffusion effects, as in the normal wave [13]. The minimum value of  $f(\text{Ar})$  occurs at the location, where the pressure gradient is maximum.

In contrast to the one-temperature continuum approach [14], the DSMC method allows simulating multi-temperature kinetic media. The most significant differences are found in distributions of parallel temperature  $T_X$  of species across the spherical shock wave. In supersonic flow, the effect of freezing  $T_X$  found in [13] has been confirmed. The freezing comes first for heavier molecules (Ar) at smaller values of  $Kn_*$ . The transverse temperature  $T_Y$  for both species follows the temperature in the isentropic expansion [14]. In all considered cases of similarity parameters,  $T(\text{He})$

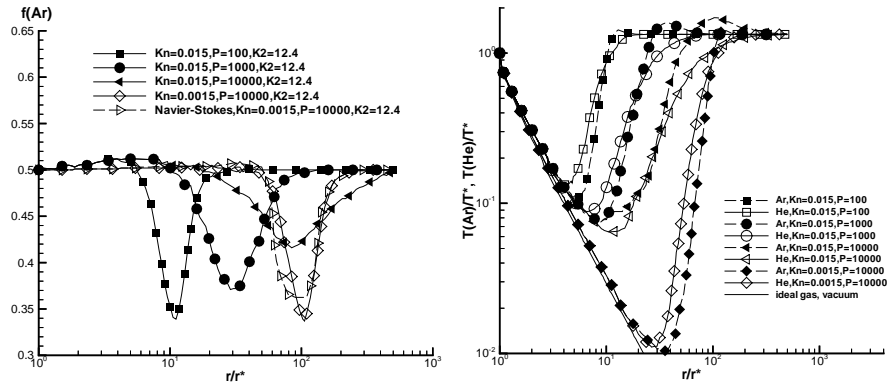


**Fig. 3** *Left*: Argon mole fraction distributions and *Right*: species temperatures in spherical expanding flow of Ar-He mixture at different Knudsen numbers  $Kn_*$  and pressure ratios  $P$

increases more rapidly than  $T(\text{Ar})$  in the supersonic part of the shock wave. The situation is reverse in the subsonic zone at  $r > R_a$ , where the gap between species temperatures increases with decreasing rarefaction parameter  $K_2$  (see Fig. 3 (*right*)).

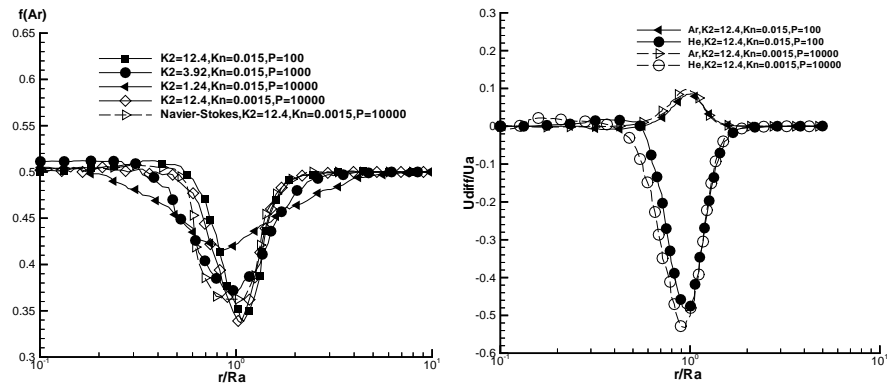


**Fig. 4** *Left*: Argon mole fraction distributions and *Right*: diffusion velocities of argon and helium in a spherical shock wave at different values of rarefaction parameters  $K_2$  and  $Kn_*$

Similarity analysis [12] is used to study the flow structure in the area behind the spherical shock. For  $K_2 = 12.4$  ( $Kn_a = 0.17$ ), light-component accumulation occurs in the spherical shock (see Fig. 4 (*left*)), as in the normal wave [13]. The DSMC data correlates with solutions of Navier-Stokes equations [14]. The pressure ratio significantly influences the shock-wave thickness, which can be measured differently by using species distributions (see Fig. 4 (*left*)), pressure, diffusive velocities (see Fig. 4

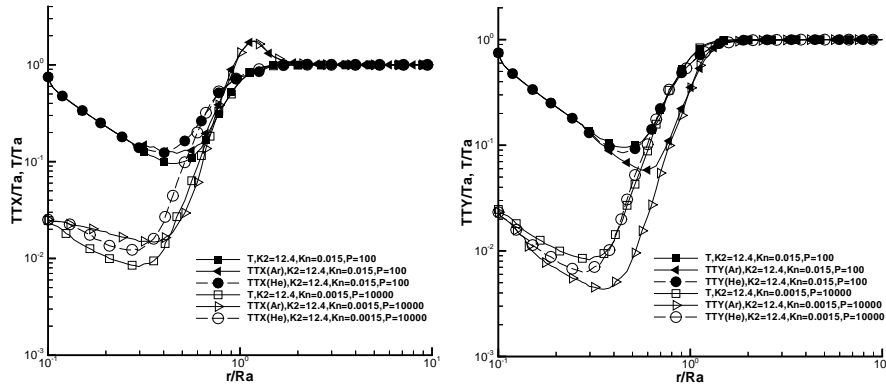


**Fig. 5** *Left*: parallel and *Right*: transverse temperatures of argon and helium in a spherical shock wave at different values of rarefaction parameters  $K_2$  and  $Kn_*$ .

(*right*)), parallel (see Fig. 5 (*left*)) and transverse temperatures (see Fig. 5 (*right*)). The flow pattern changes significantly in the shock and behind it at small values of  $K_2$ . For  $K_2 = 1.24$  ( $Kn_a = 1.7$ ), the diffusion zone is wider than in the latter case. Multi-temperature flow regime inside the shock is identified. However, the mixture enrichment with the heavy component inside the wave front, described in [14] by means of the continuum concept, was not observed.

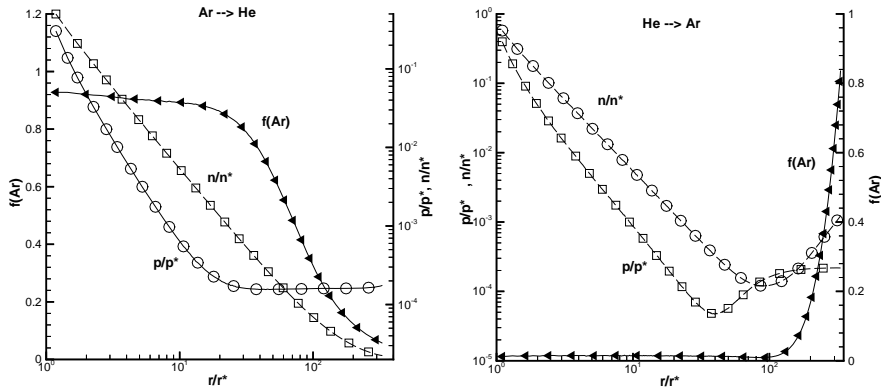


**Fig. 6** Argon mole fraction, pressure and number density in expansion of argon into helium at  $Kn_* = 0.014$  and  $K_2 = 0.785$  (*left*) and helium into argon at  $Kn_* = 0.003$  and  $K_2 = 4.53$  (*right*)

The spherical expansion of a binary gas mixture into a flooded space was analyzed in the case of the presence of a diffusive flux at the infinity  $r \gg R_a$ . The numerical results were calculated for the case of the expansion of Ar with little He

content ( $f_{Ar,*} = 0.99$ ) into a space filled by He with a small admixture of Ar ( $f_{Ar,a} = 0.02$ ). The distributions of argon concentration  $f_{Ar}$ , number density, and pressure at  $Kn_* = 0.014$ ,  $Re_* = 78.5$ , and  $K_2 = 0.785$  are shown in Fig. 6 (*left*).

The case of the expansion of He with a little content of Ar ( $f_{Ar,*} = 0.011$ ) into a space filled by Ar with small admixture of He ( $f_{Ar,a} = 0.9$ ) was also analyzed. The distributions of argon concentration  $f_{Ar}$ , number density, and pressure at  $Kn_* = 0.03$ ,  $Re_* = 453$ , and  $K_2 = 4.53$  are shown in Fig. 6 (*right*). The results demonstrate that in both cases the background gas does not penetrate through the shock wave into the inner supersonic region of the flow. In the considered cases the continuum approach is not applicable in the flow area behind the shock waves.

## 4 Conclusion

The group of similarity parameters ( $Kn_*$ ,  $Kn_a$ ,  $K_2$ ,  $B_*$ ,  $Re_*$ , and  $Re_a$ ) was found to identify the rarefaction and relaxation flow regimes in spherically expanding gas flows. The relaxation effects play a significant role in "freezing" rotational temperature in the supersonic zone and in estimating the shock wave width. The diffusive effects are significant for estimation of the effectiveness of species separation and ambient gas penetration. They result in "freezing" parallel temperature of species in the supersonic zone; in enriching flow with the light (He) component in the shock wave (with the maximum enrichment at  $r = R_a$ ), and in increasing the parallel temperature of the heavier (Ar) component there. The rarefaction parameter  $K_2$  is the major criterion for simulating flows in this area. The discussed phenomena and the results of previous studies [14], [15] were used for estimating flow parameters and axisymmetric jet structures in various aerodynamic applications [4].

## References

1. P.V. Marrone: *Phys. Fluids* **10**, 3 (1967)
2. B.N. Borzenko, N.V. Karelov, et al.: *J. Appl. Mech. Techn. Phys.* **17**, 5 (1976)
3. V.V. Riabov: *Uch. Zap. TsAGI* **9**, 5 (1978)
4. V.V. Riabov: *J. Aircr.* **32**, 3 (1995)
5. I.V. Lebed, V.V. Riabov: *J. Appl. Mech. Techn. Phys.* **20**, 1 (1979)
6. I.V. Lebed, E.E. Nikitin: *Dokl. Akad. Nauk SSSR* **224**, 2 (1975)
7. J.G. Parker: *Phys. Fluids* **2**, 4 (1959)
8. I.V. Lebed, V.V. Riabov: *J. Appl. Mech. Techn. Phys.* **24**, 4 (1983)
9. V.V. Riabov: *J. Thermophys. Heat Transf.* **14**, 3 (2000)
10. V.N. Gusev, A.V. Zhbakova: *Uch. Zap. TsAGI* **7**, 4 (1976)
11. V.N. Gusev, V.V. Mikhailov: *Uch. Zap. TsAGI* **1**, 4 (1970)
12. V.N. Gusev, T.V. Klimova, V.V. Riabov: *Fluid Dyn.* **13**, 6 (1978)
13. G.A. Bird: *Molecular Gas Dynamics and the Direct Simulation of Gas Flows* (Oxford University Press, London 1994)
14. V.N. Gusev, V.V. Riabov: *Fluid Dyn.* **13**, 2 (1978)
15. V.V. Riabov: *J. Thermophys. Heat Transf.* **17**, 4 (2003)